

ORIGINAL RESEARCH ARTICLE

Synthesis of titania fibers by electrospinning and its photocatalytic degradation properties

Yan Lv¹, Feng Chen¹, Yuanzheng Tang¹, Zhigang Chen^{1,2*}

¹School of Chemistry, Biology and Materials Engineering, SUST, Suzhou 215009, China

²Jiangsu Key Laboratory of Environmental Functional Materials, Suzhou 215009, China. E-mail: czg@ujs.edu.cn

Abstract

The electrospinning precursor solution was prepared by dissolving polyvinyl pyrrolidone as template, tetrabutyl titanate as titanium source, and acetic acid as inhibitor. The TiO₂ nanofibers were prepared by precursor solution electrospinning and subsequent calcination. Thermal gravimetric analysis (TG), scanning electron microscopy (SEM), X-ray powder diffraction (XRD), and transmission electron microscopy (TEM) were used to characterize and analyze the samples. The influence of technological parameters on spinning fiber morphology was also studied. The results indicate that the TiO₂ nanofibers morphology is good when the parameters are as follows: voltage 1.4×10^4 V, spinning distance 0.2 m, translational velocity 2.5×10^{-3} m·s⁻¹, flow rate 3×10^{-4} m³·s⁻¹, and needle diameter 3×10^{-4} m. The diameter of the fibers is about 150 nm. With the 1×10^{-4} mol·L⁻¹ methylene blue solution used as simulated degradation target, the degradation rate is 95.8% after 180 minutes.

Keywords: Titania; Electrospinning; Morphology; Structure; Photocatalytic Degradation

ARTICLE INFO

Received: 17 February 2021

Accepted: 8 April 2021

Available online: 15 April 2021

COPYRIGHT

Copyright © 2021 Yan Lv, *et al.*

EnPress Publisher LLC. This work is licensed under the Creative Commons Attribution-NonCommercial 4.0 International License (CC BY-NC 4.0).

<https://creativecommons.org/licenses/by-nc/4.0/>

1. Introduction

In recent years, the environmental problems caused by the rapid development of industrialization have become increasingly serious. Dyes are widely used in many industries, but they are not fully discarded. The water and soil pollution caused by waste dyes has caused serious harm to human health and ecosystem^[1]. At present, there are many methods to treat dye wastewater, the more common ones are adsorption method, membrane separation method, microbial degradation^[2], electrochemical method, etc.^[3] Among them, photocatalytic degradation technology has the characteristics of low cost, high efficiency, low energy consumption and environment-friendly, so it has developed rapidly^[4].

Among many semiconductor photocatalysts, titanium dioxide is favored for its stable chemical performance, strong oxidation ability, low price, easy availability, non-toxic and harmless and no secondary pollution in the process of organic degradation^[5]. At present, the degradation of organic pollutants by using titanium dioxide as photocatalyst has gradually shifted from experimental research to the development of practical products^[6]. The photocatalytic degradation process is divided into two steps: adsorption and photochemical reaction. Only when organic matter is adsorbed to the material surface can photocatalytic degradation be carried out. Therefore, the photocatalytic degradation

efficiency is closely related to the adsorption performance of materials to organic molecules and their photocatalytic ability. Nowadays, nano titanium dioxide photocatalytic materials include nano powder and nano film^[7]. For nano powder, although the particles are fine and easy to combine with organic matter in solution, agglomeration will occur, which will make the catalyst inactive, thus reducing the photocatalytic efficiency. Moreover, the nano particles are difficult to separate and recover, which is not conducive to the regeneration and reuse of the catalyst. Although nano films are easy to recover and recycle, their practical application is limited because of their small specific surface area and low photocatalytic efficiency. The film composed of one-dimensional titanium dioxide nanofibers can not only be recycled, but also improve the photocatalytic performance by increasing the specific surface area of the nano film. Wu Mingchung, Andra Sapi *et al.* synthesized palladium modified titanium dioxide composite nanofibers through cellulose/catalyst composite system, which greatly improved the photocatalytic performance of the materials^[8]. Electrospinning technology is the only one method that can directly and continuously prepare nanofibers^[9,10]. This is a spinning method to obtain nano fibers by spray stretching of polymer solution or melt under electrostatic action. It has the advantages of simple equipment, strong operability and high efficiency and has played an important role in many fields such as nano fiber preparation^[11]. The process parameters affecting the spinning were studied by electrospinning, and anatase titanium dioxide films mainly composed of fibers with a diameter of about 150 nm were synthesized^[12]. The fibers are disorderly and cross arranged, and have certain toughness. The crystal structure and micro morphology were studied by XRD, SEM and TEM. The material has high photocatalytic activity and is not easy to inactivate. The advantages of morphology and structure make it reusable and easy to separate and recover. The photocatalytic performance of methylene blue solution was studied by degrading it under ultraviolet light.

2. Experiment

2.1 Raw material

Tetra-n-butyl titanate ($C_{16}H_{36}O_4Ti$, chemically pure), absolute ethanol (analytically pure), glacial acetic acid (analytically pure), all of which are produced by Sinopharm Chemical Reagent Co., Ltd. Polyvinylpyrrolidone (PVP, analytical purity, $M_w = 1,300,000$, Aladdin Reagent Co., Ltd.), self-made deionized water, P25 powder (nano titanium oxide, Degussa, Germany, with an average diameter of about 20 nm).

2.2 Preparation

Weigh 2 g of polyvinylpyrrolidone (PVP) with molecular weight of 1.3 million, fully dissolve it in 40 ml of absolute ethanol, drop 2 ml of glacial acetic acid to keep the solution acidic, and stir at room temperature for 3 h. Transfer 3.7 ml of tetra-n-butyl titanate with a pipette gun and add it slowly, and then stir at room temperature for 6 h to prepare a slightly viscous light yellow transparent spinning solution. Use a 5 ml disposable medical syringe to suck a certain amount of spinning solution and install it on the SS electrospinning machine. First set the injection speed, injection distance, left-right translation speed of the nozzle and the distance between the nozzle and the plane receiving steel plate, turn on the LED observation lamp, apply high voltage at the nozzle through the high-voltage DC power supply, and adjust the voltage through the knob. Make the spinning fiber form Taylor cone pattern. In the spinning process, the nozzle is required to have neither spinning liquid accumulation nor spinning splash. After spinning, the obtained nanocomposite fiber material was placed in a vacuum drying oven for 6 hours, the temperature is set at 40 °C to remove the residual solvent. Then, the fiber was calcined to 600 °C in muffle furnace at 5 °C·min⁻¹ for 1 h to prepare nano-TiO₂ fiber film material.

2.3 Characterization and testing

It was characterized by thermogravimetric analysis (TG) and differential scanning calorimetry (DSC). The test conditions are: heating rate

20 °C·min⁻¹, air flow 2 × 10⁻³ L·s⁻¹, the injection amount is about 2 mg, and the temperature range is 25–800 °C. S-4800 field emission scanning electron microscope (FESEM) of Hitachi was used to observe the morphology of the samples. The powder was identified by D8 X-ray diffraction (XRD) produced by Bruker company. The prepared nano materials were analyzed by X-ray diffraction (XRD). The XRD measurement parameters were: CuK α radiation line, filtered by curved graphite crystal monochromator, working voltage 40 kV, working current 40 mA, scanning speed 5°·min⁻¹. The particles were observed by JEM-2100 transmission electron microscope (TEM) made in Japan, and the working voltage was 200 kV. The preparation concentration is 300 ml of 1 × 10⁻⁴ mol·L⁻¹ methylene blue solution, add 0.1 g of sample, stir magnetically in the dark for 60 min to establish the adsorption balance between dye and catalyst, and put it into the photocatalytic reaction device for reaction. The light source is four 15 W UV lamps. The constant temperature is 30 °C, and in the same proportion, P25 is also placed in the photocatalytic reaction device for reaction. Take samples at every certain time, centrifuge and take the supernatant. Measure the concentration after degradation with a spectrophotometer to obtain the degradation rate of dyes. Degradation rate = [(initial concentration – post-degradation concentration)/initial concentration] × 100%.

3. Results and discussion

3.1 Thermogravimetric analysis

Figure 1 is the TG-DSC diagram of the composite obtained after electrospinning. From **Figure 1**, it can be observed that there is an obvious weight loss process of the sample before 100 °C accompanied by the endothermic of the system, which is the desorption of H₂O physically adsorbed on the sample surface and the volatilization of residual solvent. There are two obvious exothermic peaks at about 380 °C and 516 °C, and the exothermic peak near 380 °C is due to the oxidation and decomposition of n-tetrabutyl titanate to form titanium dioxide in air. PVP began to decompose at 400 °C, and there was

a significant exothermic peak at 516 °C, and PVP completely decomposed near 550 °C. After 600 °C, the weight and heat flow curve of the sample will not decrease. In order to obtain pure titanium dioxide, the calcination temperature of the material can be set to 600 °C.

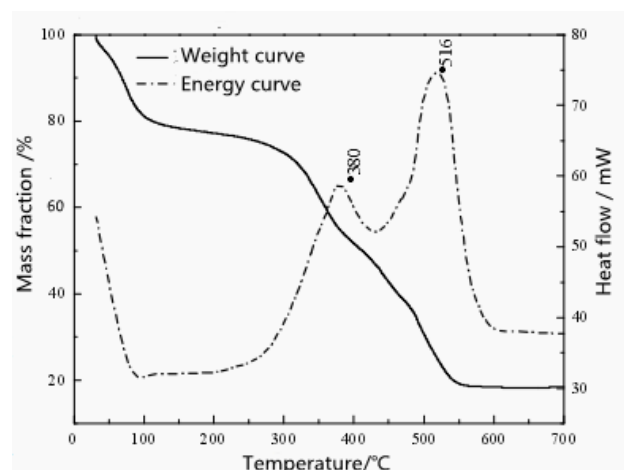


Figure 1. TG-DSC diagram of PVP/tetra-n-butyl titanate spinning film.

3.2 Exploration on the best spinning process

The titanium dioxide nanofiber film prepared by electrospinning has snow white, slightly ductile, flake and no cracks. The micro fiber morphology is affected by the spinning process, including voltage, spinning distance, nozzle translation speed, jet speed, needle inner diameter and so on. Through the control variable method, the five variables are regulated, and the micro morphology of the sample is analyzed by scanning electron microscope. The more uniform the fiber distribution, the smaller the diameter, the better the material morphology. And there is no fracture and adhesion, so as to obtain the best spinning process.

3.2.1 Voltage effect

Take the voltage as the variable, and the other variables remain unchanged. At 8 × 10³ V, 1.4 × 10⁴ V, 2.5 × 10⁴ V, the samples were spun to obtain SEM photos (**Figure 2**). **Figure 2(a)** shows voltage at 8 × 10³ V, the fiber thickness is uneven and beads appear. **Figure 2(b)** shows voltage at 1.4 × 10⁴ V, the fiber thickness is uniform, and the fiber surface is smooth and continuous. **Figure 2(c)** shows voltage at 2.5 ×

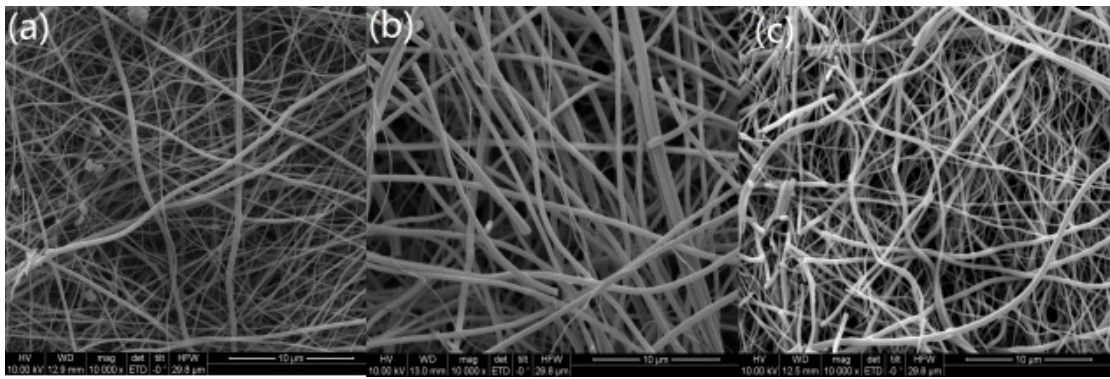


Figure 2. SEM of titanium dioxide film at positive voltage of 8×10^3 V (a), 1.4×10^4 V (b), 2.5×10^4 V (c).

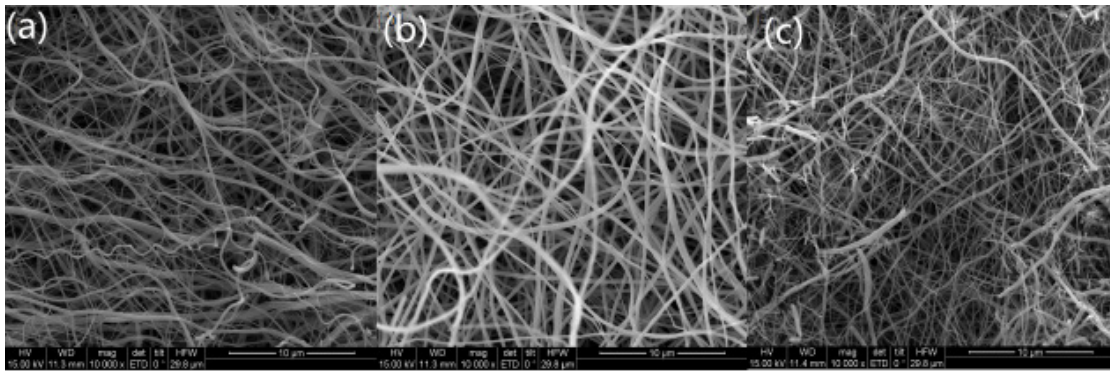


Figure 3. SEM of titanium dioxide film at spinning distance of 0.15 m (a), 0.2 m (b) and 0.25 m (c).

10^4 V, the fiber is fine, messy, and a large number of fractures occur. From this analysis, in **Figure 2(a)**, when the spinning voltage is too low, the formed electric field force is small, but to overcome the surface tension of the solution, the electrostatic field force is insufficient, resulting in that the spinning solution cannot be stretched into silk in time, so beads are formed. In **Figure 2(c)**, when the voltage is too high, during jet operation, the electric field is strong, so that the fibers are pulled very thin and disorderly, and even some fibers are pulled off. Therefore, it is necessary to select an appropriate voltage so that the electrostatic field force can overcome the surface tension of the solution without being too large to break the fiber. In **Figure 2(b)**, when the positive voltage is 1.4×10^4 V, the spinning is not only uniform in thickness, but also free of beads and fracture, and the morphology is intact. To sum up, when the voltage is 1.4×10^4 V, the spinning effect is the best.

3.2.2 Influence of spinning distance

The spinning distance is the distance between the spinning needle and the receiving plate. Take the spinning distance as the variable, keep the rest unchanged, and set the receiving distance as 0.15 m, 0.2 m and 0.25 m, then the samples were spun, and the SEM photos of the samples were obtained (**Figure 3**). It can be analyzed that the spinning distance has an obvious effect on the uniformity of fiber thickness. The change of curing distance mainly affects the electric field strength and whether the solvent in the fiber can volatilize completely. In **Figure 3(a)**, when the spinning distance is 0.15 m, the spinning distance is short, so that the fiber cannot be fully stretched, the thickness of the spinning fiber is uneven, and some filaments are thicker, so as to form a large number of curls. The solvent cannot be fully volatilized, so that the fiber can be partially bonded. In **Figure 3(b)**, when the spinning distance is 0.2 m, the distance is moderate; the fiber thickness is uniform; the arrangement is relatively orderly, and the spinning morphology is intact. In **Figure 3(c)**, when the spinning distance is 0.25 m, the spinning distance

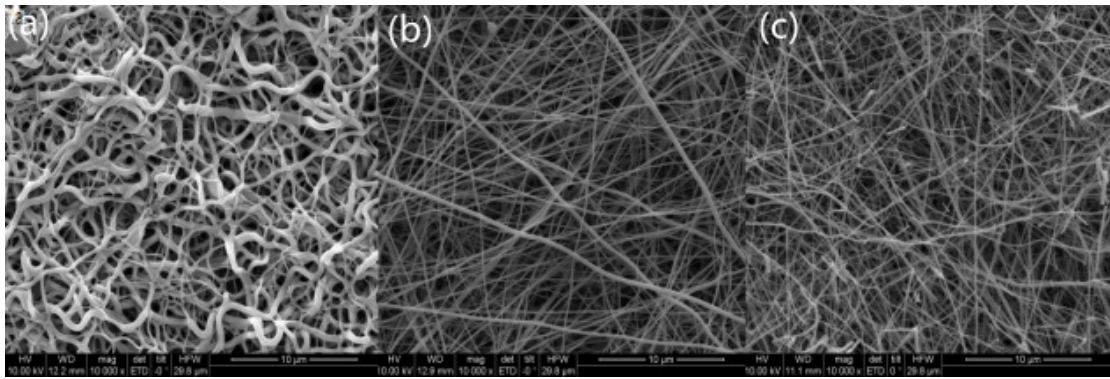


Figure 4. SEM of titanium dioxide film at nozzle translation speed of $0 \text{ m}\cdot\text{s}^{-1}$ (a), $2.5 \times 10^{-3} \text{ m}\cdot\text{s}^{-1}$ (b), $5 \times 10^{-3} \text{ m}\cdot\text{s}^{-1}$ (c).

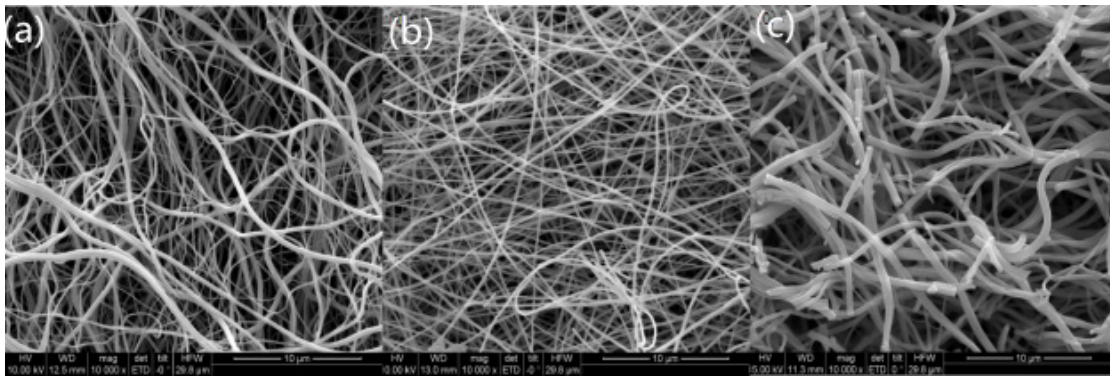


Figure 5. SEM of titanium dioxide film of pinning speed at $3 \times 10^{-4} \text{ m}\cdot\text{s}^{-1}$ (a), $5 \times 10^{-4} \text{ m}\cdot\text{s}^{-1}$ (b), $7 \times 10^{-4} \text{ m}\cdot\text{s}^{-1}$ (c).

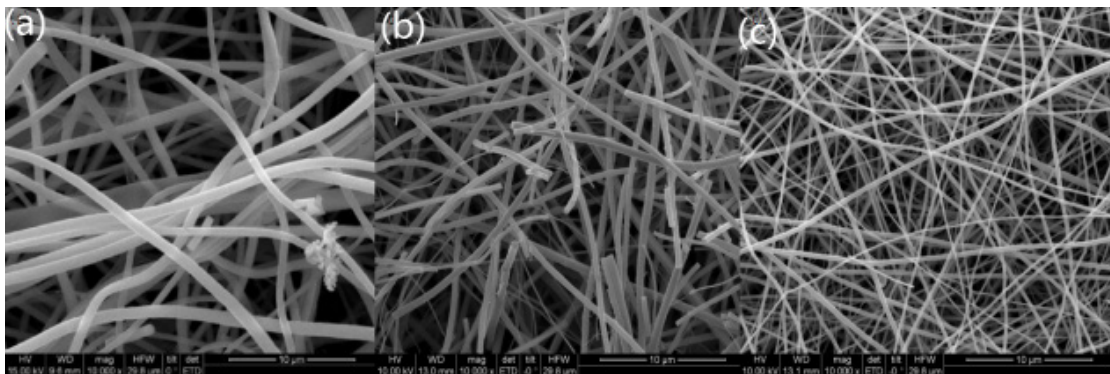


Figure 6. SEM of titanium dioxide film at the inner diameter of $7 \times 10^{-4} \text{ m}$ (a), $5 \times 10^{-4} \text{ m}$ (b), $3 \times 10^{-4} \text{ m}$ (c).

is long. Although the solvent is fully volatilized, the spun fiber cannot be received in time, and the electric field strength is relatively reduced, resulting in turbulence, and a large number of fiber fractures, more disorder and uneven fiber thickness. To sum up, the spinning distance, that is, the curing distance, is 0.2 m, the spinning effect was the best.

3.2.3 Translation speed

Taking the translational velocity of the needle as the variable, the other quantities remain unchanged. At the speed of $0 \text{ m}\cdot\text{s}^{-1}$, $2.5 \times 10^{-3} \text{ m}\cdot\text{s}^{-1}$, 5×10^{-3}

$\text{m}\cdot\text{s}^{-1}$ respectively, the spinning was carried out, and the scanning electron microscope photos of the samples were obtained (**Figure 4**). As can be seen from **Figure 4**, in **Figure 4(a)**, when the needle does not move, for no longitudinal traction, the fibers accumulate was in a fixed position, so the fibers are curled and the diameter is too large. In **Figure 4(b)**, when the needle translation speed is $2.5 \times 10^{-3} \text{ m}\cdot\text{s}^{-1}$, the spinning is smooth, fiber is uniform thickness and intact morphology. In **Figure 4(c)**, when the translation speed is $5 \times 10^{-3} \text{ m}\cdot\text{s}^{-1}$, the needle moves rapidly left and right, causing partial fracture of the

fiber. It can be analyzed that the translation speed has a significant impact on the fiber morphology. In order to control the phenomenon of fiber curling and fracture, it is necessary to select the appropriate translation speed. To sum up, the translation speed is set to $2.5 \times 10^{-3} \text{ m}\cdot\text{s}^{-1}$, the spinning effect was the best.

3.2.4 Jet speed

Taking the injection speed as the variable, the other quantities remain unchanged. At the speed of $3 \times 10^{-4} \text{ m}\cdot\text{s}^{-1}$, $5 \times 10^{-4} \text{ m}\cdot\text{s}^{-1}$, $7 \times 10^{-4} \text{ m}\cdot\text{s}^{-1}$, the samples were spun to obtain SEM photos (**Figure 5**). In **Figure 5(a)**, when the injection speed is $3 \times 10^{-4} \text{ m}\cdot\text{s}^{-1}$, the spinning is continuous, smooth, uniform, without fracture, and the fiber is fine. In **Figure 5(b)**, when the injection speed is $5 \times 10^{-4} \text{ m}\cdot\text{s}^{-1}$, the spinning is relatively uniform and partial fracture occurs. In **Figure 5(c)**, when the injection speed is $7 \times 10^{-4} \text{ m}\cdot\text{s}^{-1}$, the spinning fiber is thicker and has accumulation. It can be analyzed that the spinning speed has a significant impact on the diameter of the fiber. From **Figure 5(a)** to **Figure (c)**, the diameter of the fiber is gradually increasing with the increase of the jet speed, because the jet amount per unit time is increased with the increase of the jet speed, and the Taylor cone receiving surface formed by spinning is relatively fixed, so the tensile degree of the electrostatic field on the spinning solution must be reduced. Moreover, in the spinning process, the spinning liquid will accumulate in the needle due to the large injection volume and failure to spin in time. Of course, the smaller the jet speed, the better. If the amount is too small, there will be spinning discontinuity and fiber disconnection. To sum up, the injection speed is set to $3 \times 10^{-4} \text{ m}\cdot\text{s}^{-1}$, then the spinning effect was the best.

3.2.5 Needle size

The needle size is variable, and the other quantities remain unchanged. Under the inner diameter of $7 \times 10^{-4} \text{ m}$, $5 \times 10^{-4} \text{ m}$, $3 \times 10^{-4} \text{ m}$, the samples were spun to obtain SEM photos (**Figure 6**). In **Figure 6(a)**, when the needle of inner diameter $7 \times 10^{-4} \text{ m}$ is selected, the prepared fiber is thicker and the fiber is

not straight. Select the needle of inner diameter $5 \times 10^{-4} \text{ m}$ in **Figure 6(b)**, the prepared fiber is uniform in thickness, but slightly broken. Select the needle of inner diameter $3 \times 10^{-4} \text{ m}$ in **Figure 6(c)**, the prepared fibers are evenly distributed and the fiber diameter is much thinner. It can be analyzed that the thickness of the needle will also affect the diameter of the spinning fiber, because the thickness of the inner diameter of the needle directly affects the amount of spinning jet. From **Figure 6(a)** to **Figure 6(c)**, as the needle becomes thinner, the prepared fibers not only have small diameter, uniform distribution, but also have intact morphology. Therefore, the fiber prepared by selecting the needle with an internal diameter of $3 \times 10^{-4} \text{ m}$ is better.

Based on the above scanning morphology of fiber film under different voltage, spinning distance, jet speed and needle inner diameter, it can be concluded that the voltage is set to $1.4 \times 10^4 \text{ V}$ for electrospinning parameters, spinning distance 0.2 m , translation speed $2.5 \times 10^{-3} \text{ m}\cdot\text{s}^{-1}$, injection speed $3 \times 10^{-4} \text{ m}\cdot\text{s}^{-1}$, needle inner diameter $3 \times 10^{-4} \text{ m}$, the titanium dioxide fiber film with the smallest fiber diameter and the best uniformity and no fracture agglomeration can be obtained. The titanium dioxide film with this morphology is the best morphology.

3.3 Structure and morphology analysis

Figure 7 is at a voltage of $1.4 \times 10^4 \text{ V}$, spinning distance 0.2 m , translation speed $2.5 \times 10^{-3} \text{ m}\cdot\text{s}^{-1}$, injection speed $3 \times 10^{-4} \text{ m}\cdot\text{s}^{-1}$ and needle inner diameter $3 \times 10^{-4} \text{ m}$ XRD pattern of titanium dioxide fiber film with the best spinning morphology prepared. Wide diffraction peaks appeared at $2\theta = 25.4^\circ$, 37.5° , 48.1° , 54.0° , 55.1° , 62.7° , 68.8° , 70.3° and 75.0° . Corresponding to the characteristic peaks of (101), (004), (200), (105), (211), (204), (116), (220) and (215) crystal planes of anatase TiO_2 , narrow diffraction peaks also appeared at $2\theta = 27.4^\circ$, 36.1° , 41.2° and 56.6° . Corresponding to the characteristic peaks of (110), (101), (111) and (220) crystal planes of rutile TiO_2 , it can be seen that the titanium dioxide synthesized by electrospinning is mainly anatase phase (JCPDS21-1272), and there is also a small amount of more stable rutile phase (JCPDS21-1276). According

to Scherrer formula, the average grain size of TiO₂ nanofibers is about 14.3 nm.

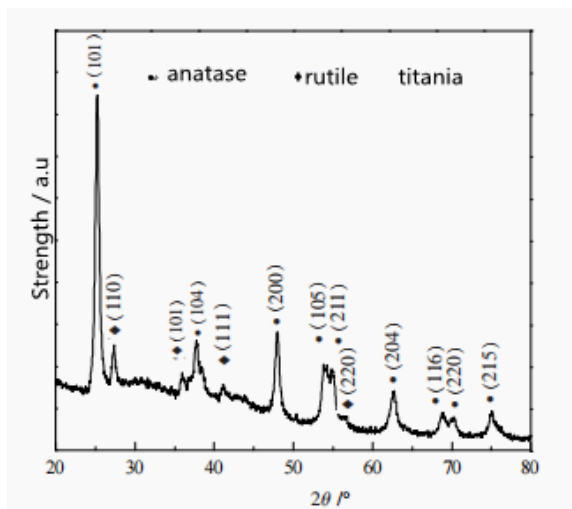


Figure 7. XRD diffraction pattern of titanium dioxide fiber film.

Figure 8 is a TEM photograph of nano titanium dioxide fiber film material at different resolutions. It can be observed from **Figure 8(a)** that titanium dioxide is fibrous, the fiber morphology is well preserved, and has a large aspect ratio. It can be seen in **Figure 8(b)** that the fiber is actually assembled from nano-sized titanium oxide particles. At the same time, it can be seen that the diameter of the fiber is about 150 nm. Under the high-power observation shown in the HRTEM photo (**Figure 8(c)**), it can be seen that there are a large number of lattice lines of titanium dioxide crystal. The measured spacing of lattice lines is 0.35 nm, which corresponds to the crystal plane of anatase phase (101), and the rutile phase is not observed due to the small amount.

3.4 Photocatalytic performance

In order to investigate the photodegradation effect of titanium dioxide fiber membrane material on common dye methylene blue solution, compare

it with P25, and the degradation rate is shown in **Figure 9**. Under the same experimental conditions, the degradation rate of methylene blue solution by titanium dioxide film was 95.8%, while the degradation rate of P25 was 66.9%. Therefore, titanium dioxide fiber membrane material has better photocatalytic activity. This is because the fluffy fiber structure of the sample makes the material have strong adsorption capacity, which makes methylene blue molecules easier to adsorb on the active sites of the material. The photogenerated hole transmission rate of titanium oxide is fast, which reduces the recombination probability of photogenerated electrons and holes, thus avoiding the rapid deactivation of the catalyst. Moreover, titanium fiber oxide surface is rich in hydroxyl group and has strong adsorption water capacity. Water and hydroxyl groups can react with surface holes to form strong oxidative hydroxy radicals, which can decompose the methyl blue solution in a short time.

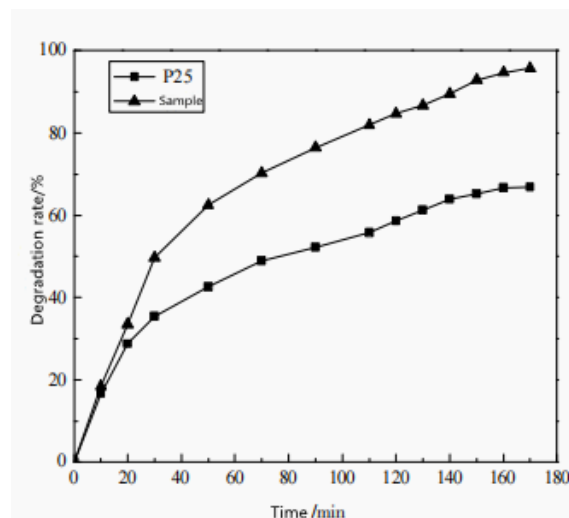


Figure 9. Degrade rate of titanium dioxide fiber membrane samples and P25 on methylene blue solution.

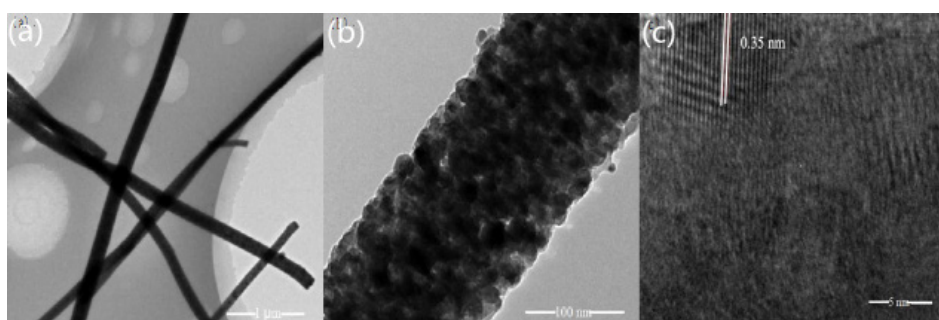


Figure 8. TEM photos of nano titanium dioxide fiber membrane material at different magnification.

4. Conclusion

PVP/tetra-*n*-butyl titanate composite nanofibers were prepared by electrospinning and calcined in a muffle furnace at 600 °C. By exploring the influencing factors of electrospinning, the optimum spinning conditions were obtained: the voltage was 1.4×10^4 V, spinning distance 0.2 m, translation speed $2.5 \times 10^{-3} \text{ m}\cdot\text{s}^{-1}$, injection speed $3 \times 10^{-4} \text{ m}\cdot\text{s}^{-1}$, needle inner diameter $3 \times 10^{-4} \text{ m}$. XRD and TEM characterization showed that the products obtained under the optimum conditions were mainly composed of anatase titanium oxide long fibers, with uniform fiber distribution and good morphological structure. The diameter of the fibers was about 150 nm. Titanium oxide grains of about 14 nm are deposited. The degradation ability of this material to methylene blue dye is much higher than that of commercial P25 titanium dioxide material, and the membrane structure of the material is more conducive to the recovery and reuse of the material, so it has great application potential.

Conflict of interest

The authors declare that they have no conflict of interest.

Acknowledgements

This work was supported by the National Natural Science Foundation of China (51478285), Natural Science Foundation of Jiangsu Province—Youth Fund (BK2014, 280) and Natural Science Foundation of colleges and universities of Jiangsu Province (16KJA430008).

References

1. Zhou Q, Zhao Y. Health impacts of typical dyes and pigments. *Journal of Environment and Health* 2005; 22(3): 229–231.
2. Lu J, Yu Z, Zhang H. Research progress in the microbial degradation of dye. *Industrial Water Treatment* 2014; 34(1): 1–4.
3. Morsi MS, Al-Sarawy AA, El-Dein WAS. Electrochemical degradation of some organic dyes by electrochemical oxidation on a Pb/PbO₂ electrode. *Desalination & Water Treatment* 2011; 26(1-3): 301–308.
4. Gumus D, Akbal F. Photocatalytic degradation of textile dye and wastewater. *Water, Air & Soil Pollution* 2011; 216(1): 117–124.
5. Ye M, Chen Z, Liu X, *et al.* Ozone enhanced activity of aqueous titanium dioxide suspensions for photodegradation of 4-chloronitrobenzene. *Journal of Hazardous Materials* 2009; 167(1-3): 1021–1027.
6. Wang L, Chen Z, Guo F, *et al.* Study on photocatalytic degradation of phenol wastewater solution by TiO₂ suspension. *Applied Chemical Industry* 2011; 40(1): 13–15, 22.
7. Chen J. Home advances in study on preparing nanosized titanium dioxide. *Guangdong Chemical Industry* 2012; 39(14): 93–95.
8. Wu M, Sapi A, Avila A. Enhanced photocatalytic activity of TiO₂ nanofibers and their flexible composite films: Decomposition of organic dyes and efficient H₂ generation from ethanol-water mixtures. *Nano Research* 2011; 4(4): 360–369.
9. Greiner A, Wendroff JH. Electrospinning: A fascinating method for the preparation of ultrathin fibers. *Angewandte Chemie International Edition* 2007; 46(30): 5670–5703.
10. Wu H, Hu L, Rowell MW, *et al.* Electrospun metal nanofiber webs as high-performance transparent electrode. *Nano Letters* 2010; 10(10): 4242–4248.
11. An B, Wang J. Electrostatic spinning research and application progress of zein fiber. *Shandong Textile Science & technology* 2016; (2): 50–52.
12. Xiao W, Zeng Y. Effects of parameters on fiber diameter in electrospinning: Experiment and numerical simulation. *Journal of Donghua University (Natural Science Edition)* 2009; 35(6): 632–638.